

AD-757 263

**THE DESIGN CONSTRUCTION, AND OPERATION
OF A CO₂-N₂-He LASER**

Clarence Vernon McIntosh, Jr.

**Naval Postgraduate School
Monterey, California**

December 1972

DISTRIBUTED BY:

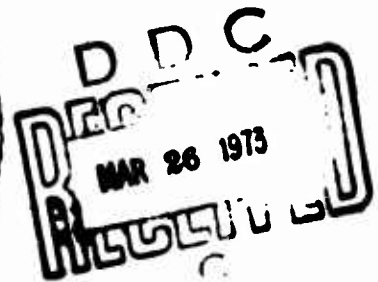
NTIS

**National Technical Information Service
U. S. DEPARTMENT OF COMMERCE
5285 Port Royal Road, Springfield Va. 22151**

AD 757263

NAVAL POSTGRADUATE SCHOOL

Monterey, California



THESIS

The Design, Construction, and Operation
of a $\text{CO}_2\text{-N}_2\text{-He}$ Laser

by

Clarence Vernon McIntosh, Jr.

Reproduced by
NATIONAL TECHNICAL
INFORMATION SERVICE
U S Department of Commerce
Springfield VA 22151

Thesis Advisor:

John P. Powers

December 1972

Details of illustrations in
this document may be better
studied on microfiche

Approved for public release; distribution unlimited.

DOCUMENT CONTROL DATA - R & D

(Security classification of title, body of abstract and indexing annotation must be entered when the overall report is classified)

1. ORIGINATING ACTIVITY (Corporate author) Naval Postgraduate School Monterey, California 93940		2a. REPORT SECURITY CLASSIFICATION Unclassified	
		2b. GROUP	
3. REPORT TITLE The Design, Construction, and Operation of a CO ₂ -N ₂ -He Laser			
4. DESCRIPTIVE NOTES (Type of report and, inclusive dates) Master's Thesis; December 1972			
5. AUTHOR(S) (First name, middle initial, last name) Clarence Vernon McIntosh, Jr.			
6. REPORT DATE December 1972		7a. TOTAL NO. OF PAGES 45	7b. NO. OF REFS 11
8a. CONTRACT OR GRANT NO.		8b. ORIGINATOR'S REPORT NUMBER(S)	
b. PROJECT NO.			
c.		8c. OTHER REPORT NO(S) (Any other numbers that may be assigned this report)	
d.			
10. DISTRIBUTION STATEMENT Approved for public release; distribution unlimited			
11. SUPPLEMENTARY NOTES Details of illustrations in this document may be better situated in a separate		12. SPONSORING MILITARY ACTIVITY Naval Postgraduate School Monterey, California 93940	
13. ABSTRACT A five-watt CO ₂ -N ₂ -He Laser was designed and constructed. The lasing mechanism of the CO ₂ -N ₂ -He gas mixture is reviewed. Beam characteristics and power output as a function of gas mixture parameters are presented.			

14

KEY WORDS	LINK A		LINK B		LINK C	
	ROLE	WT	ROLE	WT	ROLE	WT
1. Laser						
2. Gas Laser						
3. CO2 Laser						
4. CO2-N2-He Laser						

The Design, Construction and Operation
of a CO₂-N₂-He Laser

by

Clarence Vernon McIntosh, Jr.
Lieutenant, United States Navy
B.S., United States Naval Academy, 1967

Submitted in partial fulfillment of the
requirements for the degree of

MASTER OF SCIENCE IN ELECTRICAL ENGINEERING

from the

NAVAL POSTGRADUATE SCHOOL
December 1972

Reproduced from
best available copy.

Author

Clarence V. McIntosh, Jr.

Approved by:

John O. Powers

Thesis Advisor

Sidney A. Parker

Chairman, Department of Electrical Engineering

Milton H. Clausen

Academic Dean

TABLE OF CONTENTS

I.	HISTORY AND INTRODUCTION -----	5
II.	THE LASING MECHANISM -----	7
	A. CO ₂ VIBRATIONAL-ROTATIONAL TRANSITIONS -----	7
	B. SELECTIVE EXCITATION BY N ₂ MOLECULES -----	14
	C. AIDED DE-EXCITATION BY He -----	15
III.	SYSTEM DESIGN AND DESCRIPTION -----	16
	A. PLASMA TUBE -----	16
	B. MIRROR SYSTEM -----	16
	C. VACUUM AND GAS SYSTEM -----	22
	D. POWER SUPPLY -----	25
	E. COOLING SYSTEM -----	28
	F. BASE AND SUPPORTS -----	28
IV.	OUTPUT CHARACTERISTICS -----	30
	A. OPTIMUM GAS MIXTURE -----	30
	B. BEAM CHARACTERISTICS -----	30
	APPENDIX A OPERATING PROCEDURES -----	38
	APPENDIX B ALIGNMENT PROCEDURE -----	40
	BIBLIOGRAPHY -----	42
	INITIAL DISTRIBUTION LIST -----	43
	FORM DD 1473 -----	44

LIST OF DRAWINGS

Figure 1.	Vibrational States of the CO ₂ Molecule -----	8
Figure 2.	Partial Vibrational Energy Level Diagram of the CO ₂ -N ₂ -He Laser -----	9
Figure 3.	Vibrational-Rotational Band for the (00 ⁰ 1) → (10 ⁰ 0) Transitions of CO ₂ -----	11
Figure 4.	Boltzmann Distribution of Population Den- sities of the (00 ⁰ 1) Vibrational Level -----	13
Figure 5.	The Laser Tube Assembly -----	17
Figure 6.	Mirror and Window Mounting Detail Right End	19
Figure 7.	Mirror Mounting Details, Left End -----	20
Figure 8.	Vacuum Sealing Details -----	21
Figure 9.	Photograph of Output End Support and Mirror Mounting Details -----	23
Figure 10.	Photograph of Output End -----	23
Figure 11.	Vacuum and Gas System -----	24
Figure 12.	Dubrovin Type Vacuum Gauge -----	26
Figure 13.	Power Supply Schematic Diagram -----	27
Figure 14.	Photograph of the CO ₂ -N ₂ -He Laser System ---	29
Figure 15.	Power Output vs. CO ₂ Partial Pressure -----	31
Figure 16.	Power Output vs. N ₂ Partial Pressure -----	32
Figure 17.	Power Output vs. He Partial Pressure -----	33
Figure 18.	Power Output vs. Discharge Current -----	34
Figure 19.	Beam Cross-section at Various Distances from the Output Window -----	35
Figure 20.	Estimated Beam Diameter vs. Distance from the Output Window -----	37

I. HISTORY AND INTRODUCTION

The development of a CO₂ molecular gas laser was first published by C. K. N. Patel of Bell Telephone Laboratories in 1964 [Ref. 1]. The laser described used the molecular vibrational-rotational transitions of the electronic ground state of CO₂ to produce a CW output of about 1 mW.

Later in the same year Patel reported the observation of selective excitation of CO₂ through the transfer of vibrational energy from N₂ molecules, with resulting laser action of the CO₂ at 10.6 μ [Ref. 2]. This CO₂-N₂ system was to produce 16.2 watts [Ref. 3], a sizable increase over the pure CO₂ laser.

A further and more dramatic increase in efficiency and power output was to come the next year with the discovery that large amounts of Helium aided the CO₂ lasing process. Again reported by Patel [Ref. 3], power output in excess of 100 watts and efficiency of 6-7 percent were obtained from a device similar to the ones which had developed outputs of milliwatts with pure CO₂ and watts with a CO₂-N₂ mixture.

The ability of the CO₂ molecular laser to maintain spectral purity and spatial coherence at high efficiency in the far infrared frequency region ($\sim 10\mu$) opened up a new range of frequencies for laser experimental work and development. Extensive research has been carried out in the investigation of the CO₂ laser mechanism itself, as well as

related areas which use the CO₂ laser as an energy source [Ref. 4]. Power outputs in excess of 11 kilowatts CW [Ref. 4] and efficiencies of 15-20 percent have been realized [Ref. 5].

Perhaps the most important potential fields of applications for CO₂ lasers are infrared communications and laser radar. The atmospheric window at 8-13 μ makes the characteristic 10.6 μ radiation suitable for terrestrial and extraterrestrial communications [Ref. 5]. Recent research work on CO₂ lasers include evaluation of terrestrial and deep-space communications, as well as transverse-subsonic-flow, supersonic flow (gas dynamic lasers), thermal, high-pressure, and chemical systems [Refs. 4,6].

The purpose of this work was to design and build a laser with several watts of output with a minimum of purchased parts. The design is discussed following a review of the lasing mechanism. Experimental results from testing the laser are also included.

II. THE LASING MECHANISM

A. CO₂ VIBRATIONAL-ROTATIONAL TRANSITIONS

The lasing action of the CO₂ molecular laser originates from transitions between vibrational states within the same electronic level of the CO₂ molecule. A classical model provides an easily understood explanation of the vibrational states of the molecule and is illustrated in Figure 1 [Ref. 5]. The vibrational state is usually written in the form $(v_1v_2v_3)$, with v_1 describing the number of vibrational quanta in the symmetric stretch mode, v_2 the number of vibrational quanta in the bending mode, and v_3 the number of vibrational quanta in the asymmetric stretch mode. The bending mode (v_2) is two-fold degenerate and usually carries a superscript to indicate the degeneracy, for example, (01^10) . A vibrational energy level diagram for the CO₂-N₂-He laser is shown as Figure 2 [Ref. 7].

For each of the quantized vibrational levels there are a number of rotational levels. These states correspond to quanta of angular momentum, classically characterized by the quantum number J and differ by $h/2\pi$ in accordance with quantum-mechanical selection rules, where h is Planck's constant.

There may be transitions between rotational levels belonging to different vibrational levels; these transitions in CO₂ emit radiation at different IR wavelengths, forming

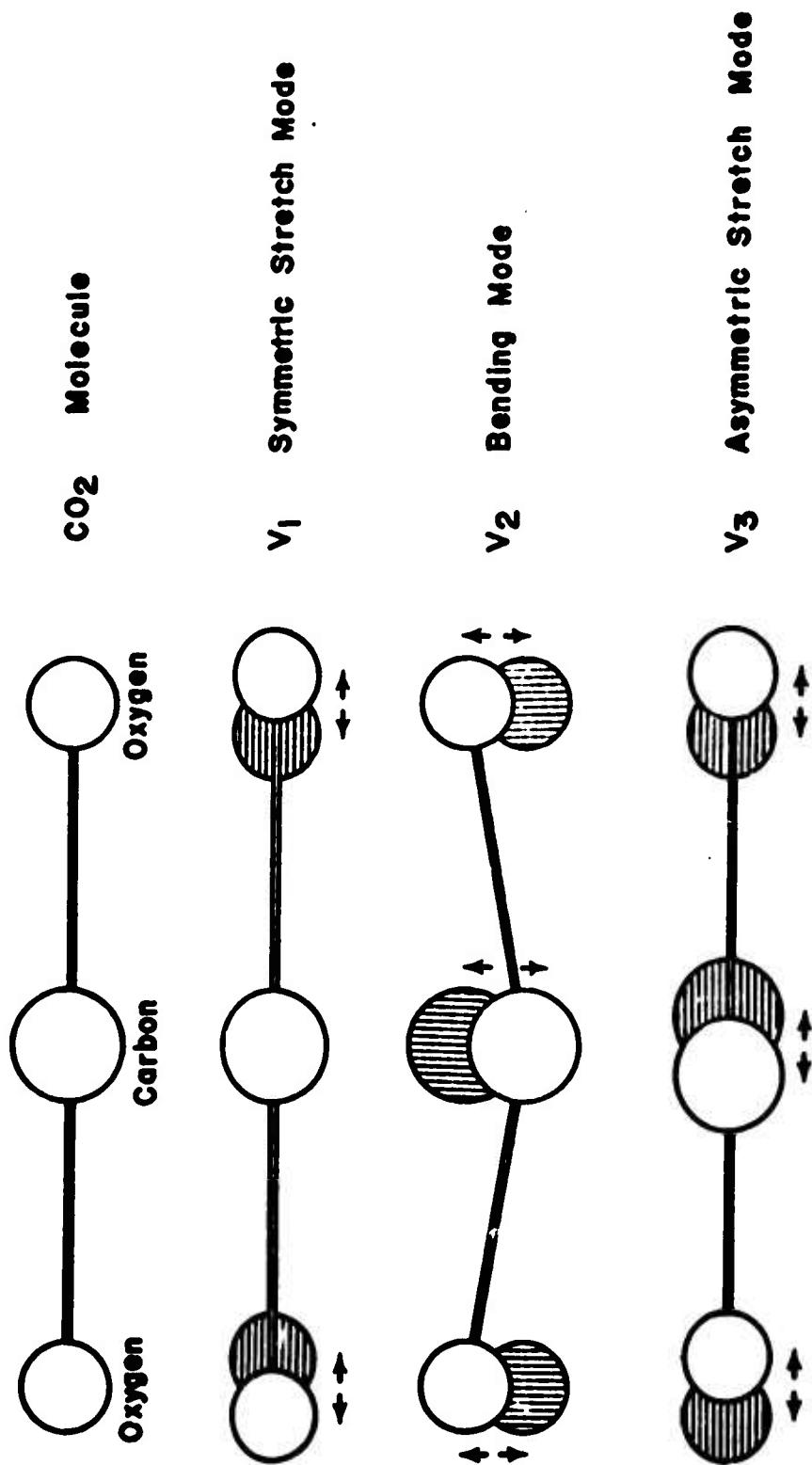


Figure 1. Vibrational States of the CO₂ Molecule (After Ref. 5)

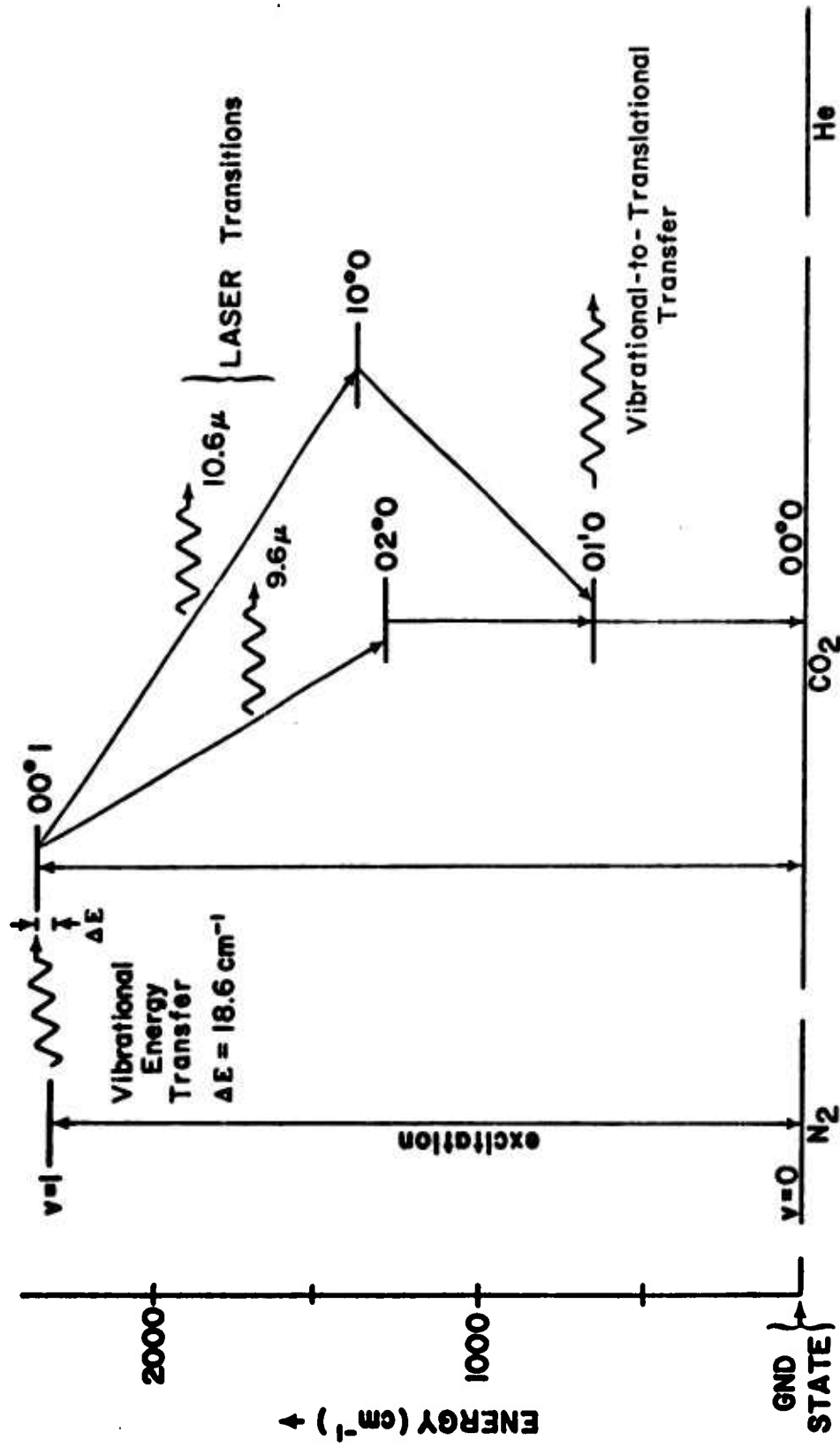


Figure 2. Partial Vibrational Energy Level Diagram of CO₂-N₂-He Laser (After Ref. 7)

what is called a vibrational-rotational band. The vibrational-rotational band for the $(00^0_1) \rightarrow (10^0_0)$ transitions which produce the 10.6μ radiation are shown in Figure 3. Symmetry considerations of the CO_2 molecule result in only odd J levels in the (00^0_1) level and even J levels in the (10^0_0) level, hence the $\Delta J=0$ transitions are not allowed. The transitions on the longer-wavelength end of the band are called P-branch transitions and the transitions on the shorter wavelength end of the band are called R-branch transitions. There are no transitions in the center of the band due to the absence of the $\Delta J=0$ transitions [Ref. 1]. Although there are many possible P and R-branch transitions within a vibrational-rotational band, a single P-branch transition will dominate all others. This is fortunate because if the laser output were to occur at a number of wavelengths the beam would not be monochromatic and its usefulness would be limited. This domination by one P-branch transition can be explained by what are called "competition effects." The energy spacings between vibrational levels are usually much greater than the kinetic energy of the molecules; the energy spacings between rotational levels, however, are smaller than the kinetic energy. thus, any and every collision can result in exchanges of energy between rotational levels and the population density of a particular rotation level will not be independent of the population density of other rotational levels within that vibrational level. The rate of this rotational

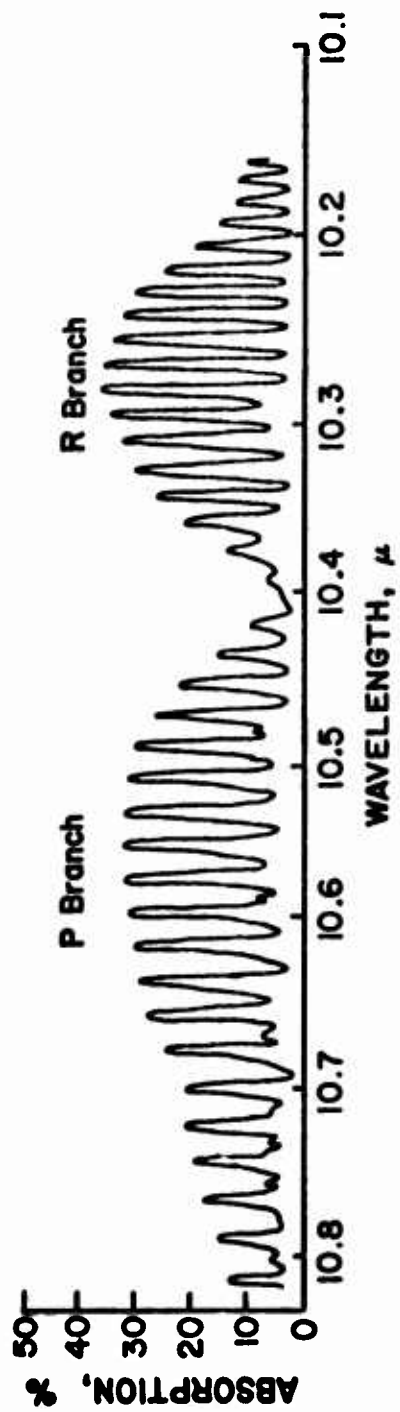


Figure 3. Vibrational-Rotational Band for the $(0001) \rightarrow (1000)$ Transitions of CO_2

(After Ref. 1)

thermalization is about 10 Mhz, whereas the vibrational thermalization rate is only about 1 Mhz. The vibrational lifetime is, therefore, about 10^{-3} seconds and the rotational thermalization time is only about 10^{-7} seconds. Accordingly, during its lifetime in a vibrational level, a molecule undergoes a large number of "hops" between rotational levels. This process gives rise to a Boltzmann distribution of molecules among the rotational levels of a vibrational level, as is shown in Figure 4. This distribution is for the (00^01) vibrational level, which is the upper laser level of the 10.6μ laser transition. The lower (10^00) laser level has a similar distribution. As the lasing action occurs, the population densities of the rotational levels of these respective vibrational levels continually adjust themselves to maintain the Boltzmann distributions. Thus, only the transition with the highest gain occurs, and it is fed at the upper level and depleted at the lower level by adjacent rotational levels. The result is an extremely coherent and monochromatic output.

The 10.6μ output from the $(00^01) \rightarrow (10^00)$ laser transition (See Fig. 2) is in the order of 10 times greater than that of the 9.6μ , $(00^01) \rightarrow (02^00)$ transition and is thus the most important output wavelength of CO_2 lasers [Ref. 5].

It should be noted at this point that the vibrational-rotational levels pertinent to the CO_2 lasing action belong to the electronic ground state of the molecule and are

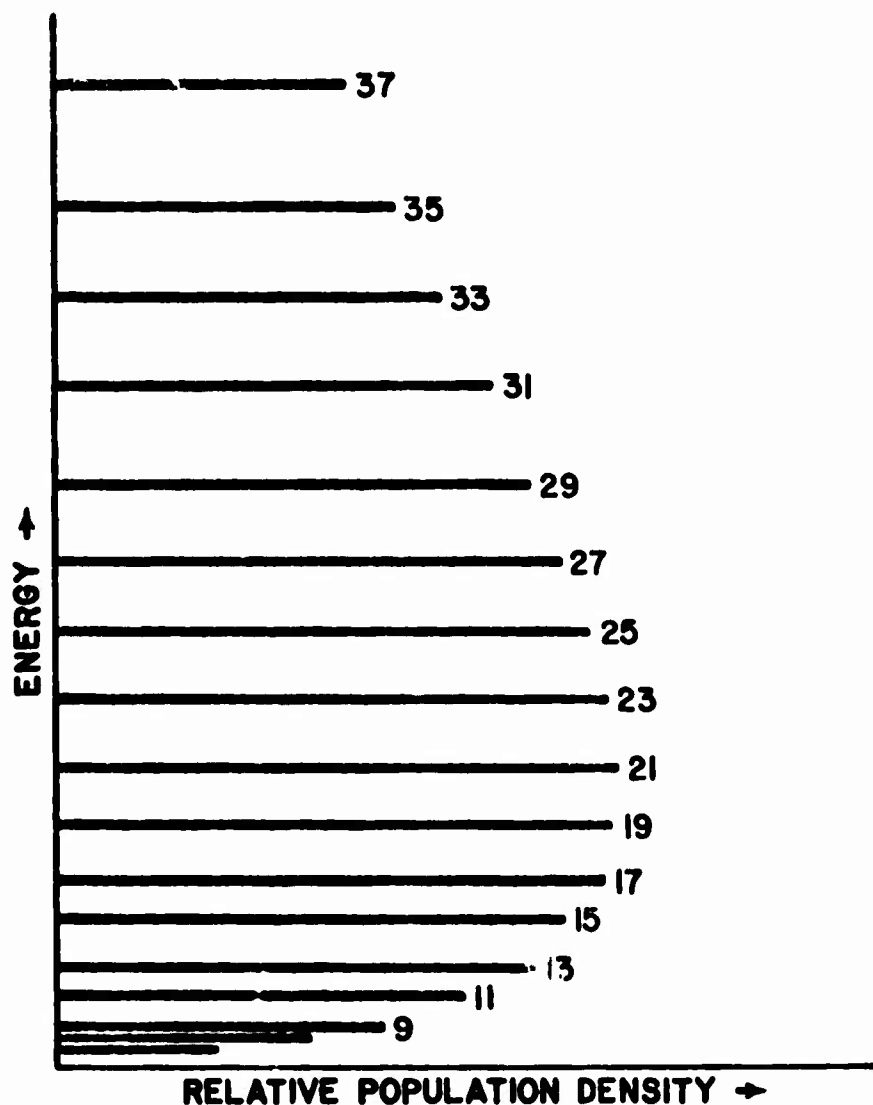


Figure 4. Boltzmann Distribution of Population Densities of the (00^0_1) Vibrational Level of CO_2 . The values indicate the value of J for each level. (After Ref. 5.)

very close in energy to the ground state. Again referring to Figure 2, it can easily be seen that the emitted laser photon energy is a sizable fraction of the total energy required to excite the molecule to the upper laser level. Also, since the energy levels are so low, almost all electrons present in a discharge will be effective in the excitation process. These facts allow high working efficiencies and thus high power outputs from CO₂ lasers [Ref. 5].

B. SELECTIVE EXCITATION BY N₂ MOLECULES

The addition of vibrationally excited N₂ molecules will greatly enhance the efficiency of a CO₂ laser by selectively exciting the CO₂ molecules to the upper laser level [Ref. 2]. The N₂ molecule has only one degree of vibrational freedom, which may be described by the quantum number v . As shown in Figure 2, the $v=1$ vibrational state is very close in energy to the CO₂ upper laser level (00⁰1). This vibrational energy is readily transferred from the N₂ (1) molecules to the CO₂ (00⁰0) molecules through collisions, elevating the CO₂ molecule to the (00⁰1) upper laser level. The higher energy states of both N₂ and CO₂ are also evenly spaced. Transfers of vibrational energy may take place at these higher levels, or the high energy molecules (either the excited N₂ or excited CO₂) may transfer one quantum of energy at a time to the ground state CO₂ (00⁰0) molecules [Ref. 5]. Thus the higher energy

molecules also participate in the overall high-efficiency of the laser action. The suitability of N_2 for use in the selective excitation of CO_2 is enhanced by its characteristic of readily exciting to the $v=1$ state in an electric discharge and its relatively long life in the excited state [Ref. 2].

C. AIDED DE-EXCITATION BY He

The efficiency and power output of CO_2 laser systems are greatly enhanced by addition of large amounts of Helium. The (10^00) and (01^10) levels are strongly coupled, but depopulation of the (10^00) lower laser level is limited by the relaxation rate of the (01^10) level [Ref. 5]. It is important that the (10^00) level be depleted quickly, since the (00^01) upper laser level has a radiative lifetime about three orders of magnitude shorter than the lower laser level [Ref. 8]. The (01^00) level is thus a "bottleneck" to efficient completion of the process. The relaxation of this level involves a vibrational-translational energy exchange with other gas molecules through collisions. Helium is the most widely used third gas for this purpose [Ref. 7]. An additional benefit is the decrease in gas temperature in an electric discharge (due to the high thermal conductivity of He [Ref. 4]). This benefit results since gas temperature has been found to be the most important plasma property of CO_2 electric discharge laser performance [Ref. 9].

III. SYSTEM DESIGN AND DESCRIPTION

A. PLASMA TUBE

The laser tube assembly is represented in Figure 5. The tube was constructed of Pyrex, and a cooling water jacket was made as an integral part of the assembly. Brass flanges are soldered to the ends of the tube in order to facilitate clamping of the assembly onto end supports. A primary design goal was to obtain several watts of CW output and it was felt that one meter of discharge length should easily realize that goal, since 50-80 watts per meter under optimum conditions have been routinely reported. Although experiments showed an inverse dependence on tube diameter for small-signal gain in CO₂ amplifiers [Ref. 11], more recent work shows output power to be relatively independent of diameter in flowing CO₂-N₂-He systems [Ref. 4]. A diameter of one inch was chosen as a matter of convenience. Gas inlet/outlet ports were provided at the ends and at the midpoint of the tube in order to permit flexibility in the choosing of gas flow arrangements. The electrodes are standard neon sign type, and are rated at 120 ma of current.

B. MIRROR SYSTEM

A relatively inexpensive, hole-coupled mirror system was used, in conjunction with a KCl output window. The

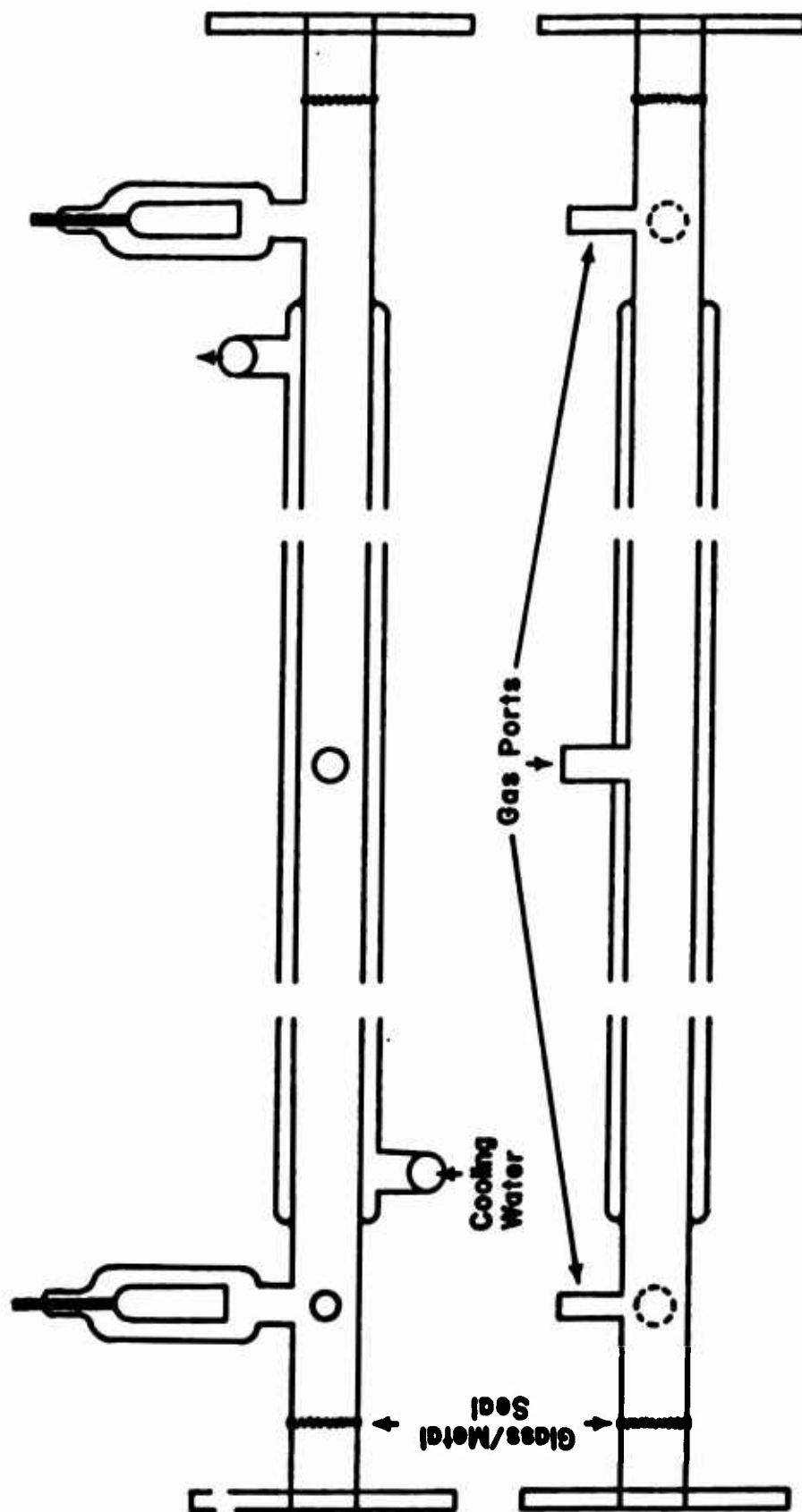


Figure 5. The Laser Tube Assembly

mirrors are gold-coated Pyrex substrates, one inch in diameter. Front surfaces are finished to $1/80$ of a wavelength at 10.6μ . The gold coating provides 98% reflectivity at 10.6μ . One mirror is flat; the output mirror is spherically concave with a 10 meter radius of curvature, and has a centered output hole, 2 mm in diameter. The mirrors were purchased from Oriel Corporation of America. The mirrors serve as the ends of the tube; there are no windows within the laser cavity. The output window is necessary in order to maintain the vacuum because of the output hole. The window is made of KCl, and is 25 mm in diameter and 5 mm thick. Flatness is $1/10$ of a wavelength at 10.6μ . KCl was chosen instead of NaCl because of its smaller absorption coefficient at 10.6μ (less than 0.01 cm^{-1} for KCl vs. 0.1 cm^{-1} for NaCl). The window was purchased from Harshaw Chemical Company. Details of the mirror and window mounting are shown in Figures 6 and 7. The mirrors are cemented into their mounts with silicone-rubber cement.

The alignment fixtures and mirror mounts are machined from aluminum, $3/8$ inch thick. The bellows material is brass and was salvaged from a bellows-type valve.

Sealing details are shown in Figure 8. A vacuum seal is maintained between machined parts by the use of neoprene O-rings in machined grooves. The bellows are mounted and sealed to the mirror alignment fixtures with epoxy cement.

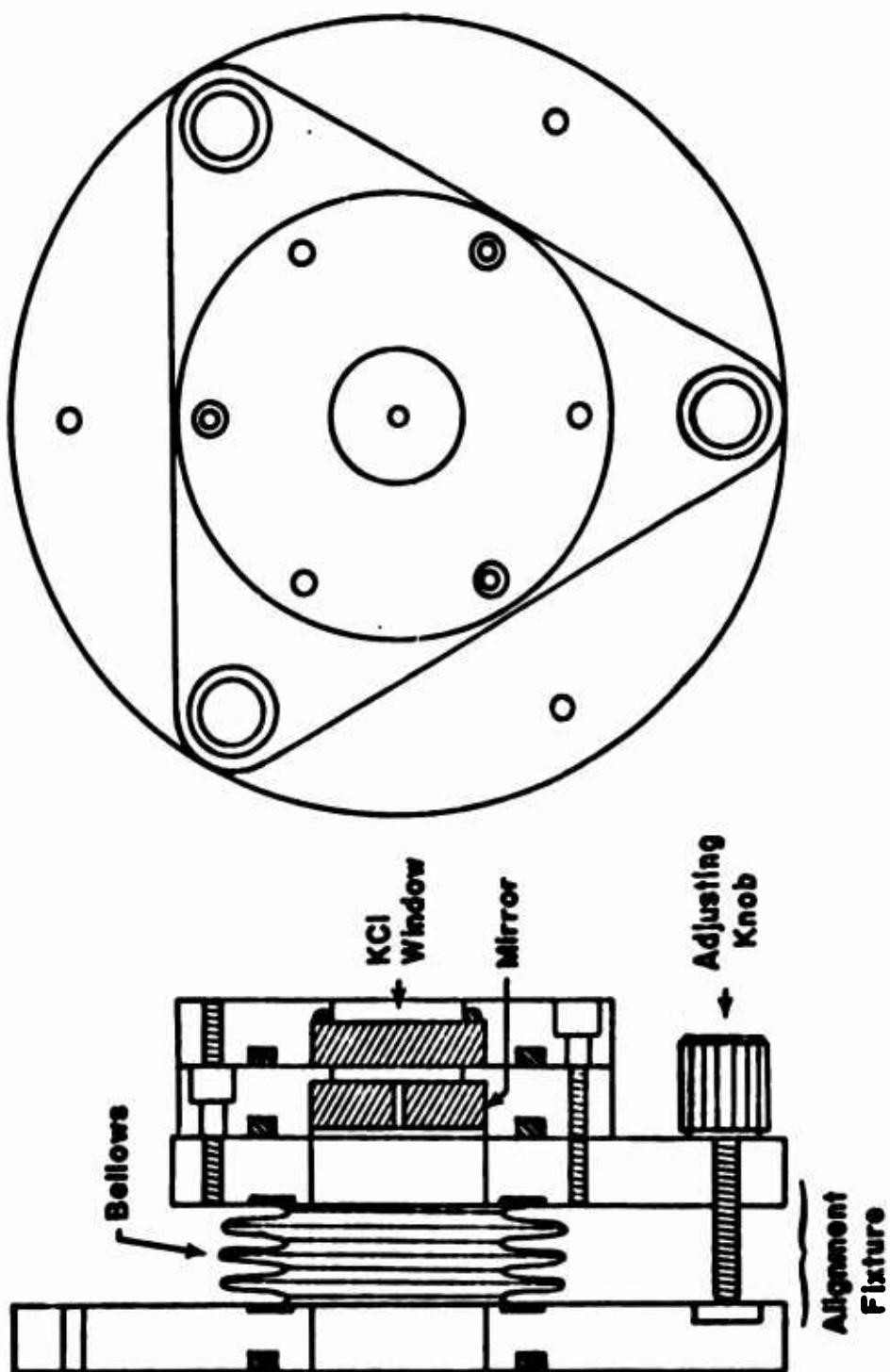


Figure 6. Mirror and Window Mounting Details, Right End

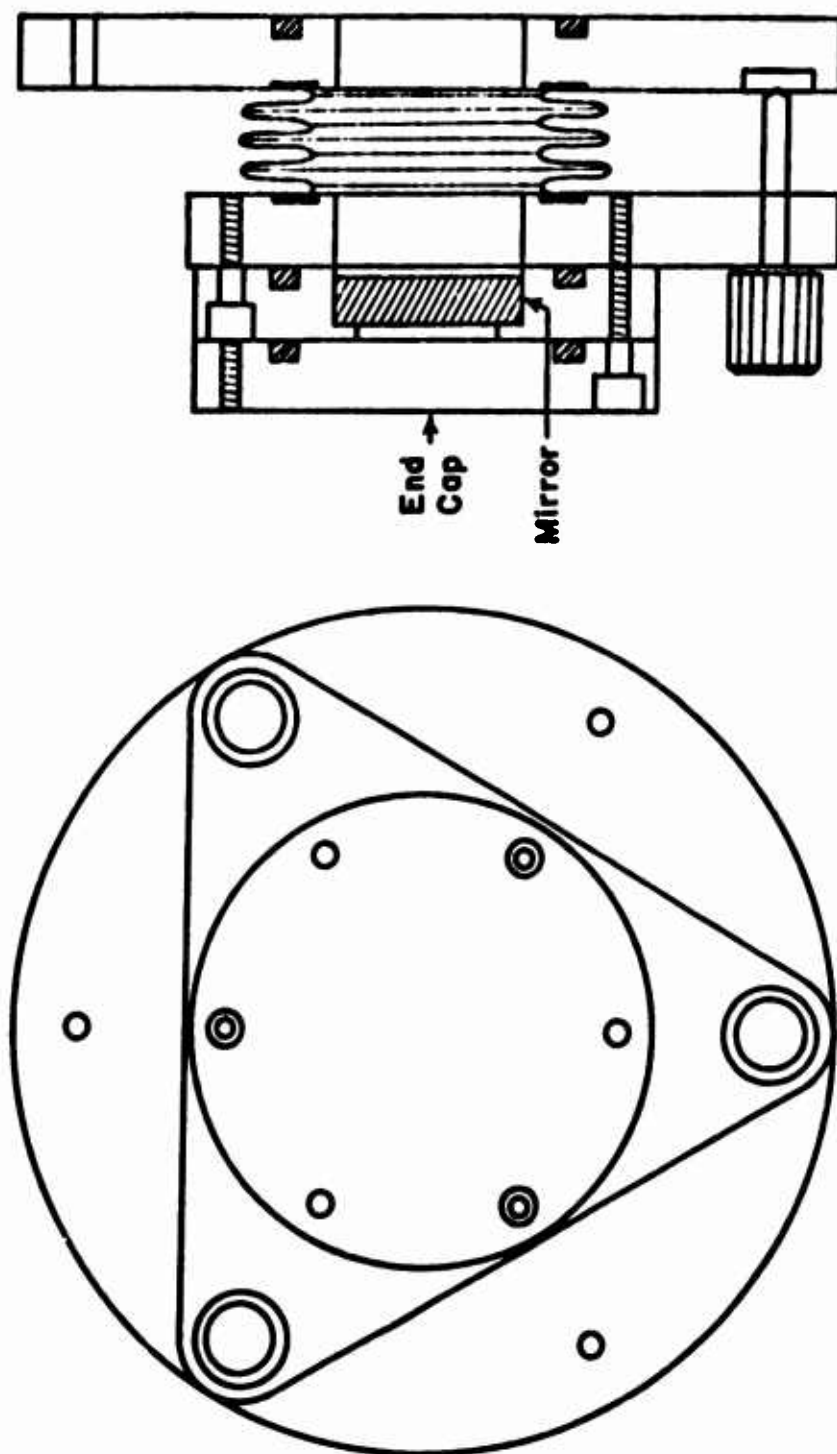


Figure 7. Mirror Mounting Details, Left End

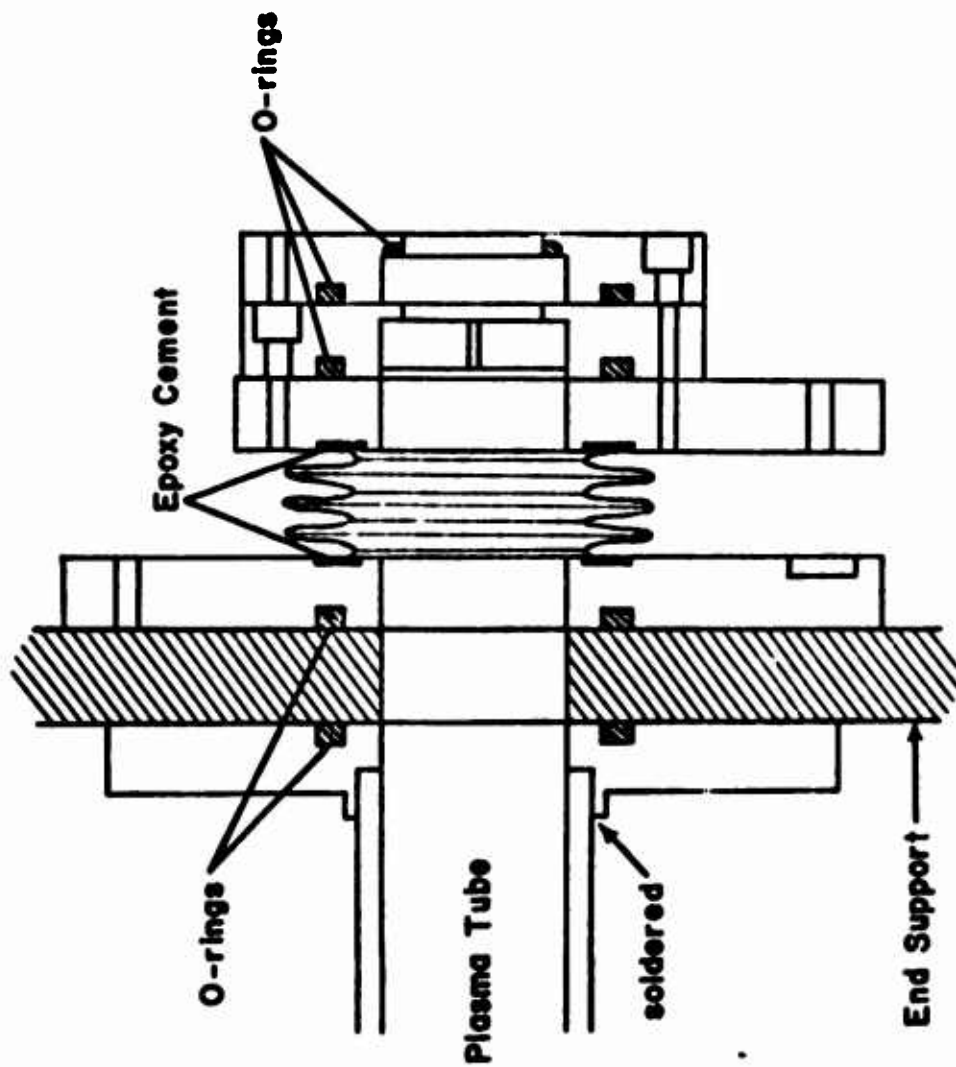


Figure 8. Vacuum Sealing Details

The output window is held securely in place and is sealed by a small O-ring.

Figures 9 and 10 are photographs of the constructed mirror mountings.

C. VACUUM AND GAS SYSTEM

The vacuum and gas system is schematically represented in Figure 11. Separate sources were supplied for CO_2 , N_2 , and He, in order that various mixture ratios and/or combinations of the gases may be utilized. The gas supply tanks are standard 200 cubic feet size (50 lbs for CO_2). A .020 inch micrometer needle-valve was installed in the CO_2 supply line to help in the regulation of the CO_2 flow, because its partial pressure is the most critical to the power output (See Ref. 4 and Sec. IV. A).

All interconnections were made with 5/16 inch (I.D.) thick-wall Tygon brand plastic tubing. The tubing was clamped to the plasma tube gas ports and to the other system components with worm-screw, automotive type hose clamps. Silicone vacuum grease was used on all connections.

A dubrovin type vacuum gauge was used. It consists of a stainless steel cylinder, closed at one end, floating vertically in a column of mercury with its open end submerged. The air is evacuated from the chamber formed by the inverted tube. An adjustable scale on the frame of the gauge is read by using the top (closed) end of the

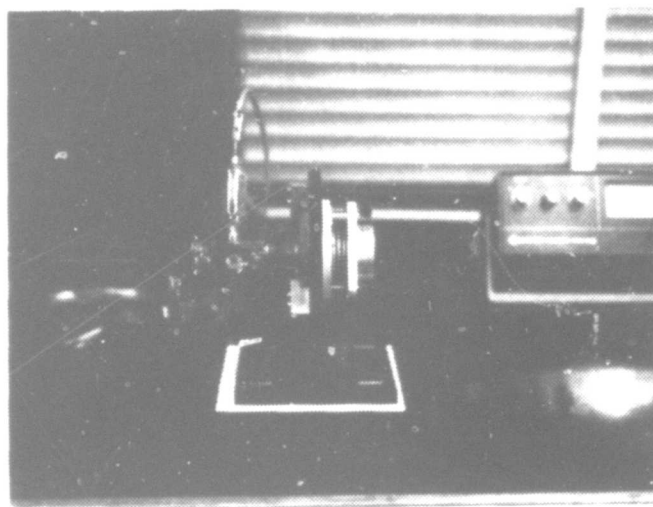


Figure 9. Output End Support and Mirror Mounting Details

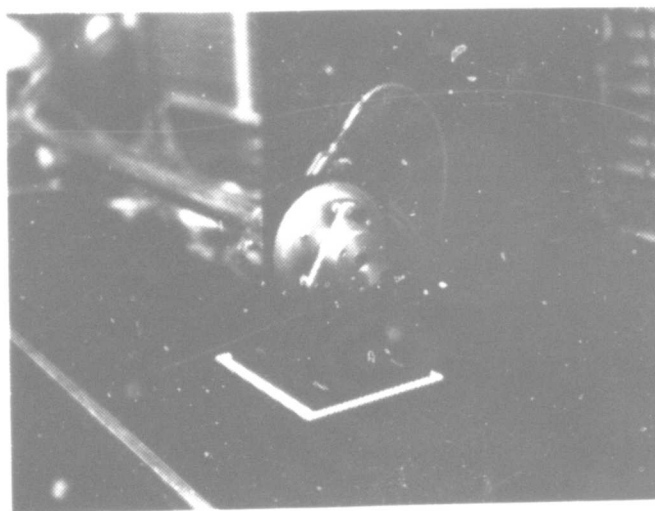


Figure 10. Output End, Showing Output Window

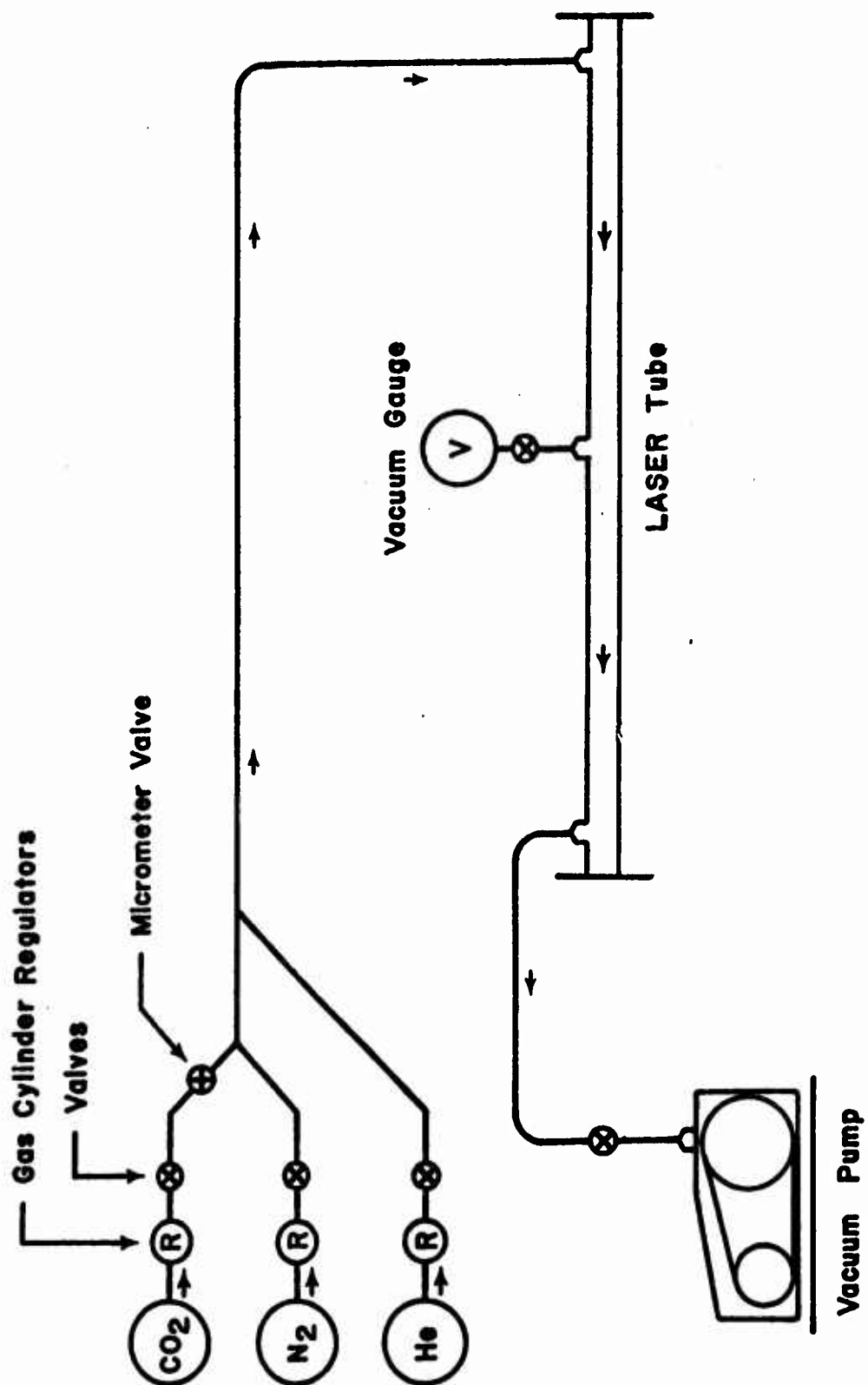


Figure 11. Vacuum and Gas System

inverted tube as an indicator. The gauge has a pressure range of from 0.2 to 20 torr (1 torr = 1 mm of mercury) in .2 torr graduations. The scale is 9x20mm in length, or 9 times as sensitive as a mercury manometer. This scale magnification factor is a function of the dimensions of the inverted tube. This gauge was found to be easy to read due to its magnified scale, and easy to use because it is not adversely affected by occasional exposure to atmospheric pressure. The physical details of the gauge are shown in Figure 12. The vacuum pump used was a standard laboratory mechanical pump.

D. POWER SUPPLY

The power supply is schematically represented in Figure 13. Its main component is a 120 v. - 12 Kv. (rms), 120 ma. luminous tube (neon sign) transformer. This type of transformer is well suited for this application because its built-in current-limiting (saturation) feature eliminates the necessity of including ballast resistance in series with the dynamic negative resistance of the discharge tube in order to prevent current runaway. A Variac autotransformer provides for continuously variable output from the secondary of 0 to 13.5 Kv. (rms). This output is then rectified in a conventional full-wave bridge of 3B24 tubes, to yield a power supply output of 0 to 19.1 Kv. (peak) or, equivalently, 0 to 12.2 Kv. (average). No filtering is

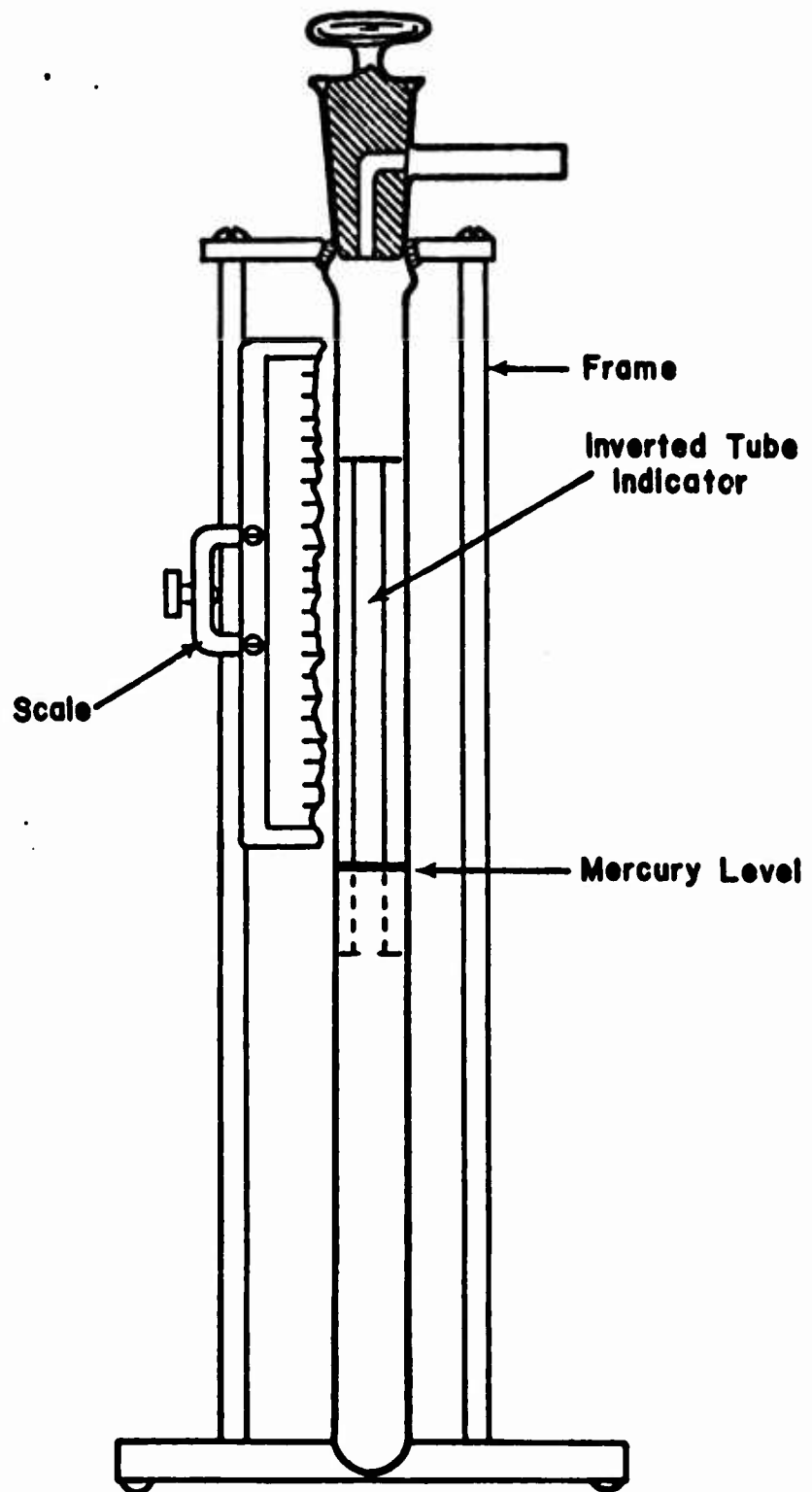
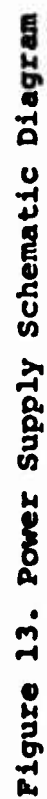


Figure 12. Dubrovin-Type Vacuum Gauge



used in the power supply output. Front-panel meters monitor output voltage and current.

E. COOLING SYSTEM

The cooling water jacket was connected to a cold water source and a drain with standard 1/2 inch (I.D.) vinyl garden hose. The hose was clamped to the water ports with automotive-type hose clamps.

F. BASE AND SUPPORTS

The laser base and end supports were machined from 1/2 inch thick aluminum plate. The supports are drilled and tapped for laser tube clamps on one side and mirror-adjusting fixtures on the other. The base plate is tapped for hold-down screws, so that the end supports can be held securely during mirror alignment. Teflon sheets, one-eighth inch thick, are placed between the end supports and the base plate during laser operation in order to prevent the discharge current from diverting through the base and supports. Wood would probably be a better choice of material for the base, and the possibility of electric shock to the laser operator would be greatly reduced.

Figure 14 is a photograph of the complete laser system.

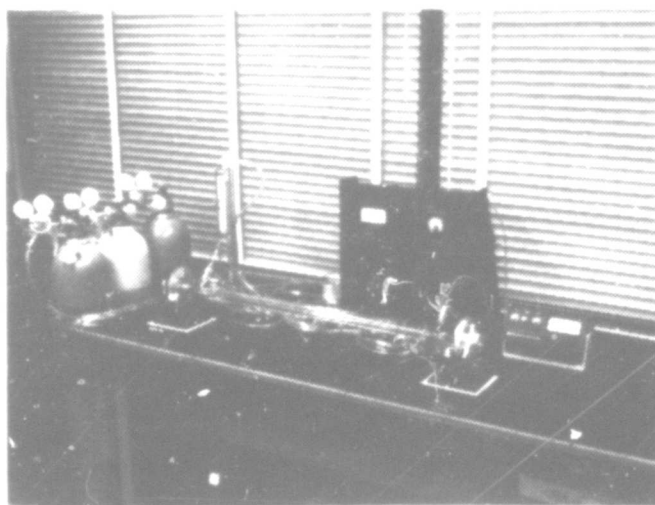


Figure 14. The CO₂-N₂-He Laser. The Output End is to the Right.

IV. OUTPUT CHARACTERISTICS

A. OPTIMUM GAS MIXTURE

The optimum gas mixture was found to be 0.9:1.6:6.0, CO₂:N₂:He. The ratio was determined by peaking the power output with each gas partial pressure until the maximum output of about 4.6 watts was attained. The power output as a function of each of the gas partial pressures is represented in Figures 15, 16, and 17. It can be seen that the power output is reduced if either CO₂ or N₂ are in excess of the amount which produces maximum laser oscillation. It can be assumed that the effect of the CO₂ is due to the absorption of light by the excess molecules. The addition of excess Helium is not detrimental to the power output once enough has been added to deplete the (01¹0) state of the CO₂. Hence the curve of Figure 17 saturates as more Helium is added. Figure 18 shows the power output as a function of discharge current.

B. BEAM CHARACTERISTICS

Cross-sectional views of the output beam were obtained by exposing sheets of IR-sensitive Thermofax paper for a few seconds at each of several distances from the output window. The exposures are shown in Figure 19. It can be seen that the beam tends to the TEM₀₁ mode at under one Meter. This effect is probably due to imperfect mirror

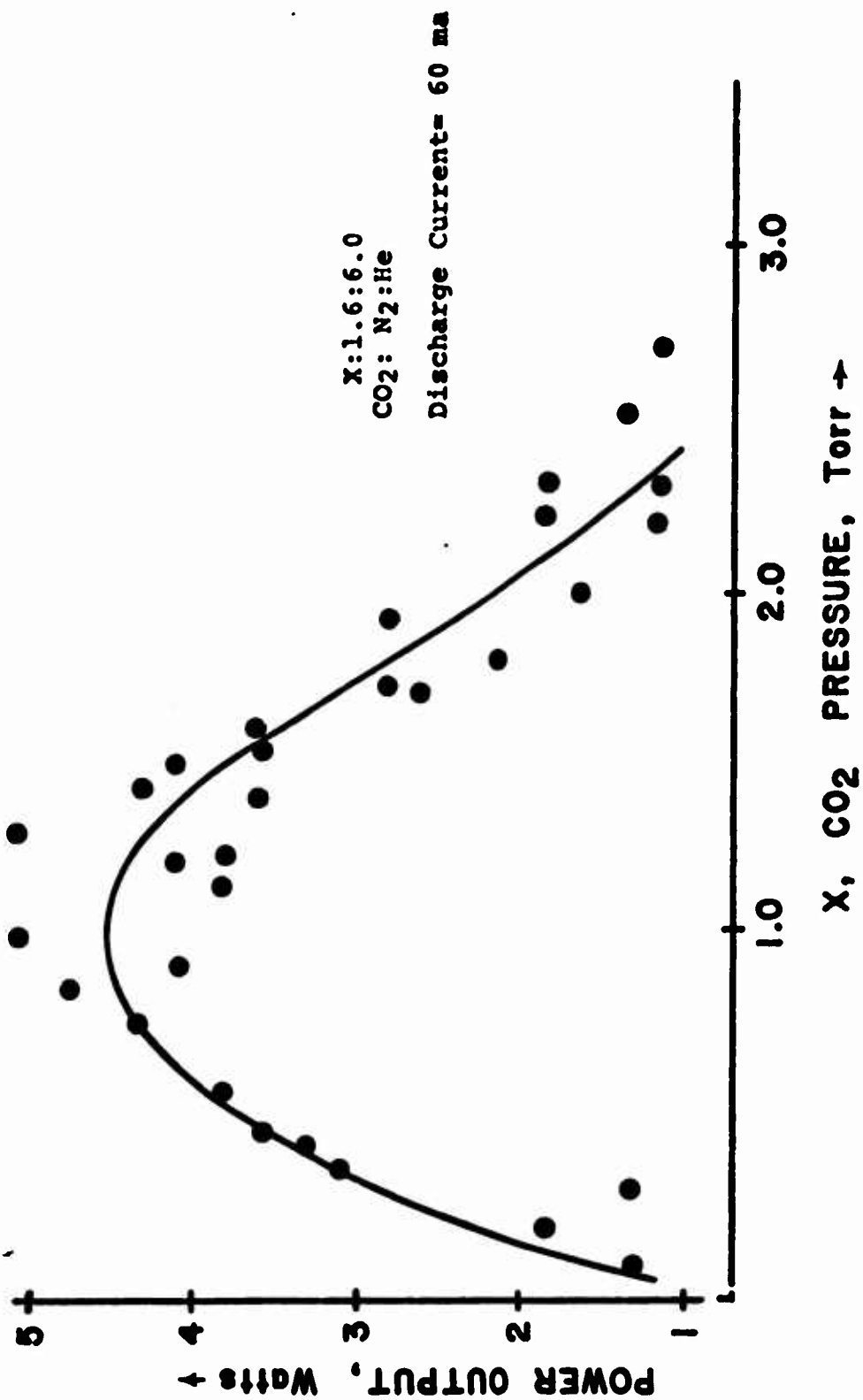


Figure 15. Power Output vs. CO₂ Partial Pressure

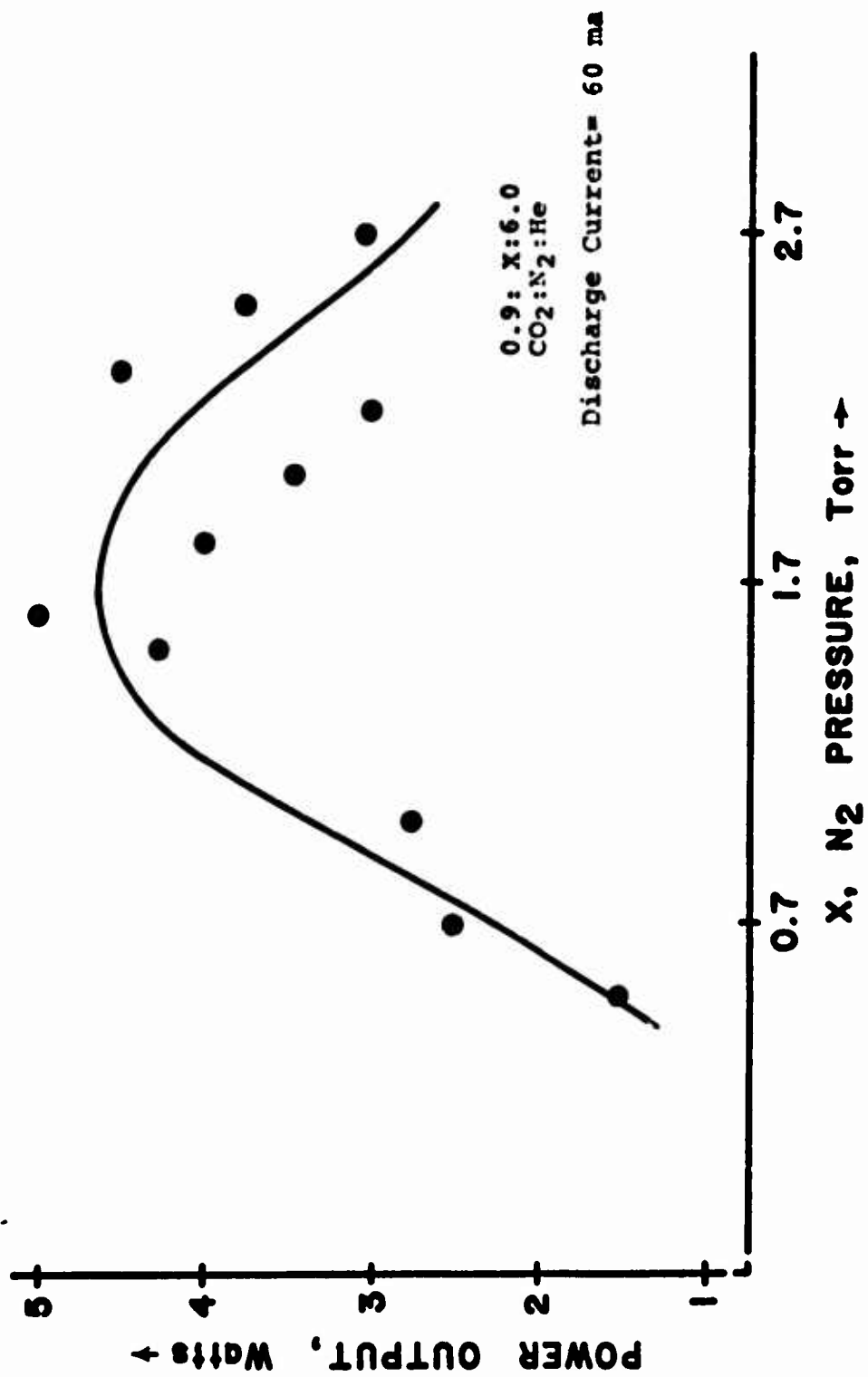


Figure 16. Power Output vs. N₂ Partial Pressure

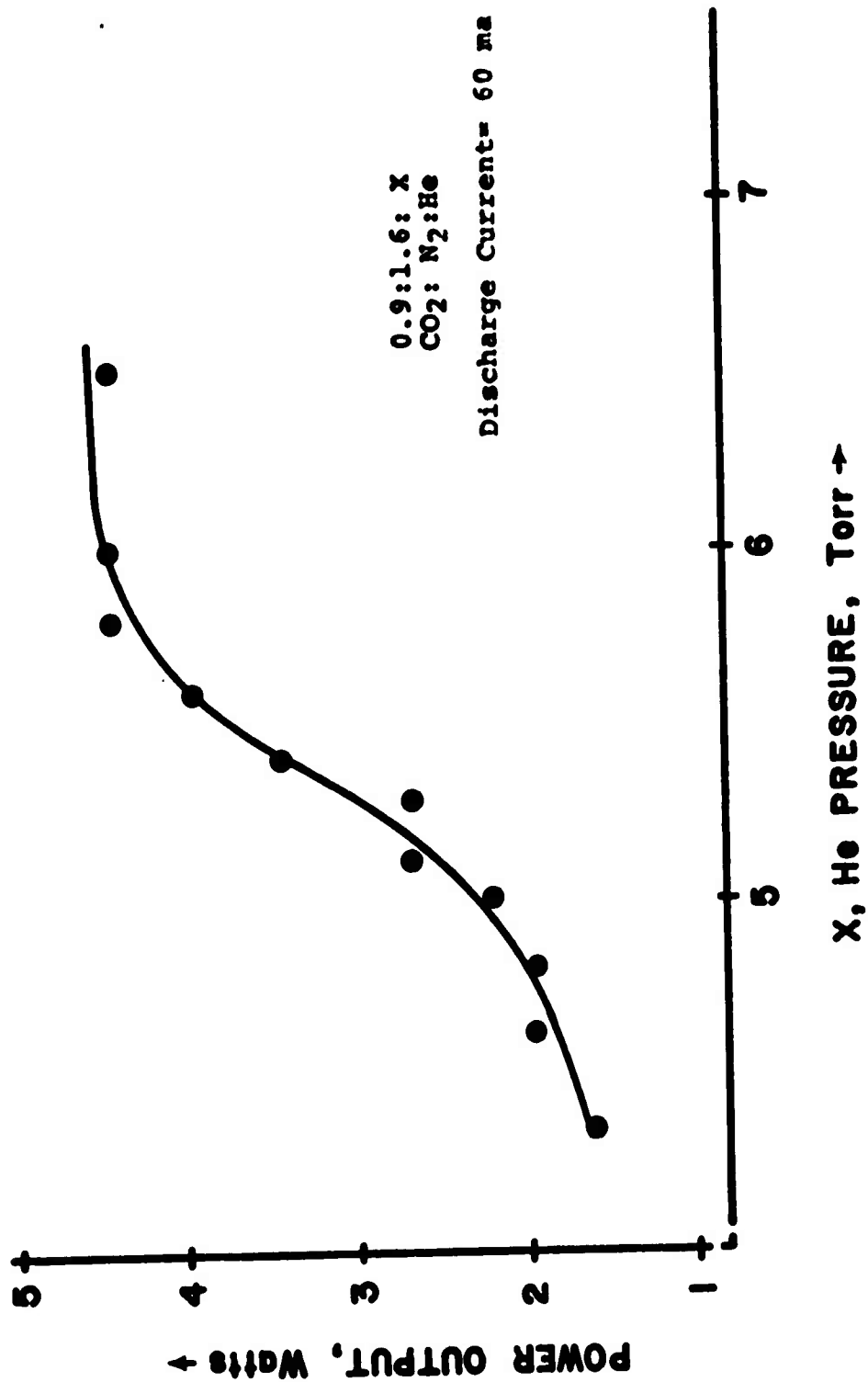


Figure 17. Power Output vs. He Partial Pressure

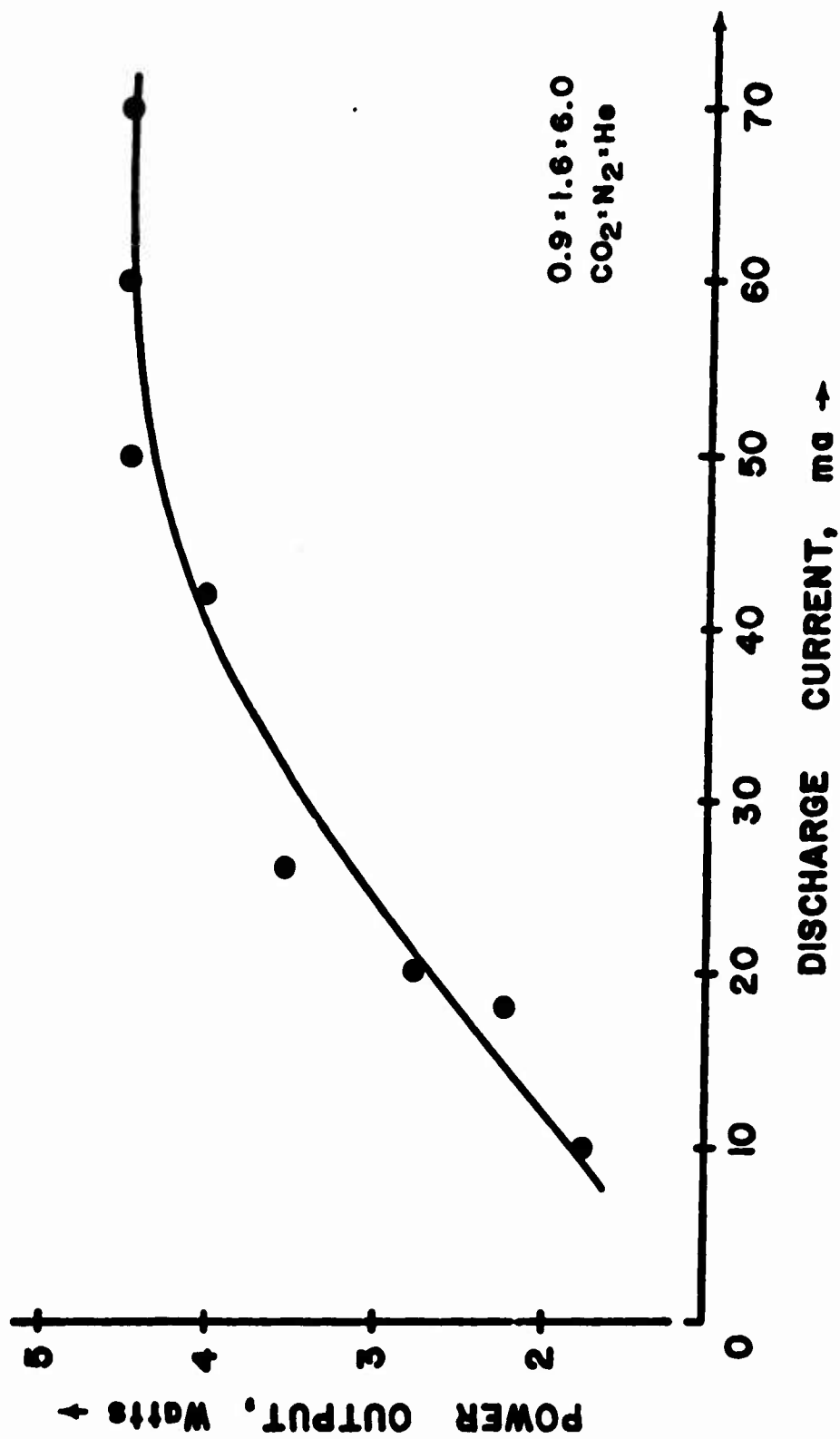


Figure 18. Power Output vs. Discharge Current

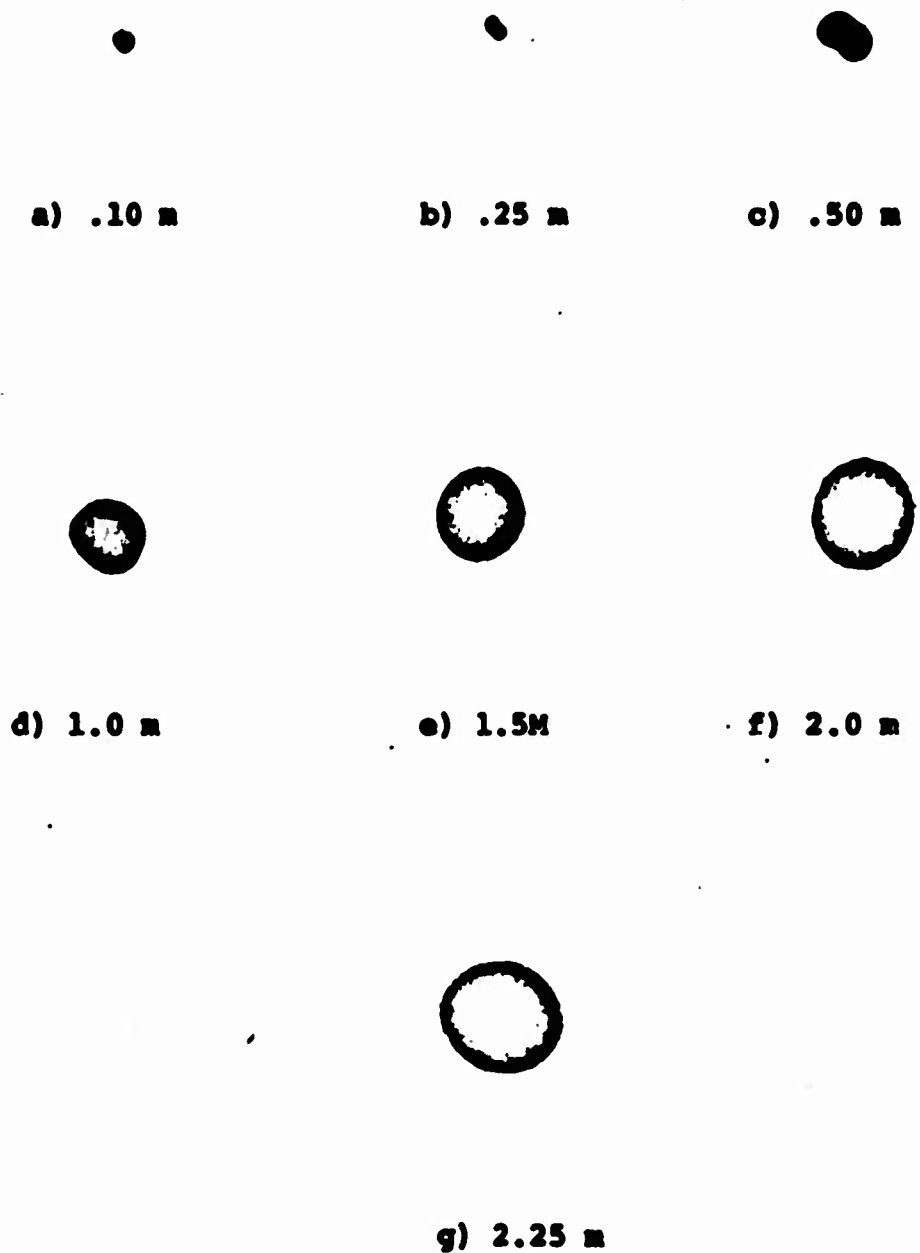


Figure 19. Beam Cross-section at various distances from the output window.

alignment. Beyond one meter the beam is the expected TEM_{00} mode. Estimated beam diameter vs. distance from the output window is shown in Figure 20. Beam expansion is shown to be approximately linear with distance. Beam divergence (full angle), as determined from the slope of the curve, is about 0.5 degrees.

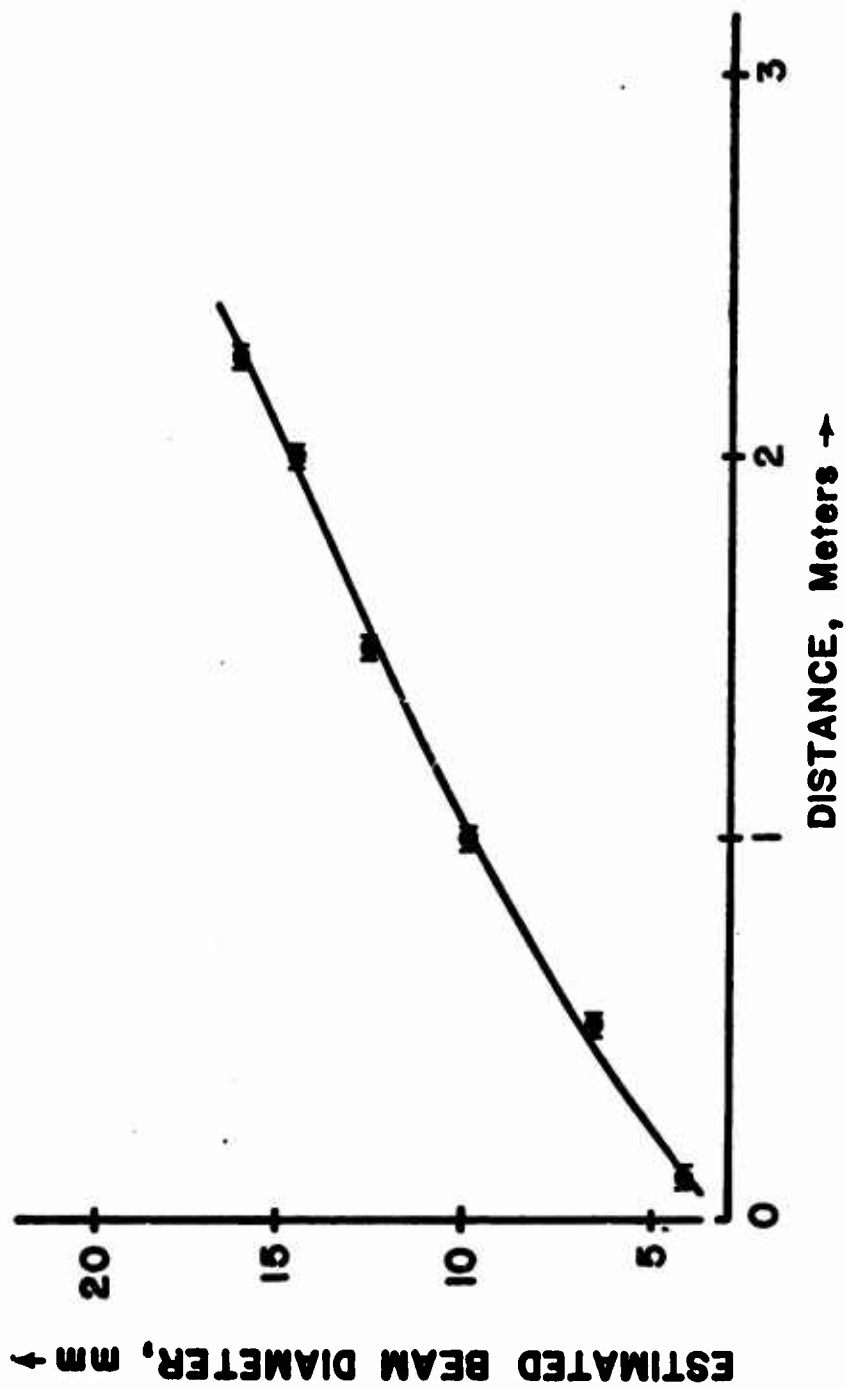


Figure 20. Estimated Beam Diameter vs. Distance

Appendix A. OPERATING PROCEDURES

1. SAFETY PRECAUTIONS

Great care must be exercised when operating the CO₂-N₂-He laser. There are extremely high voltages present on the metal parts of the laser, and the invisibility of the powerful beam compounds the danger to persons who may be unaware of its presence. Adjustments to the mirror alignment on the output end of the tube are particularly difficult; the danger exists of receiving an electric shock by touching the metal mirror mount and of putting one's fingers into the beam in an involuntary reaction to the shock. Extreme caution must be exercised in order to avoid electric shock and/or burns.

2. PROTECTION OF THE KCl WINDOW

When the laser is not in use, the vacuum pump is normally left on in order to keep the inside of the tube free of water vapor, which would soon "fog" the highly soluble KCl output window. A plastic bag containing dessicant packets is placed over the outside of the window mount to protect the window from room humidity.

3. OPERATION

The CO₂-N₂-He laser may be placed in operation as follows:

a. Cooling water, power supply filaments, vacuum pump, and detector ON.

b. Power supply output voltage control at minimum. High voltage switch ON.

c. Helium is admitted slowly by the Helium tank regulator until tube pressure is 6 to 8 torr.

d. Slowly bring up power supply output until the gas conducts. Adjust voltage for about 60 ma discharge current. The discharge will be a pink-orange color. A purple color in the discharge at this point indicates that there is a leak in the sys'em.

e. Slowly admit nitrogen by the nitrogen tank regulator until the tube pressure increases by about 1.5 to 2 torr. The discharge color will change to a deep blue. It may be necessary to increase the power supply voltage in order to maintain the gas discharge.

f. Slowly open the CO₂ supply micrometer valve to admit CO₂ into the system. The laser will begin to oscillate and the discharge color will turn to a thin blue-gray. Adjust the micrometer valve to optimize output.

g. Readjust the He and N₂ valves for optimum output.

Appendix B. ALIGNMENT PROCEDURE

1. MIRROR SYSTEM ALIGNMENT

A Helium-Neon laser is used to align the mirrors. The following procedure was used with good success:

a. Both end supports are securely fastened to the base in order to make the entire unit physically rigid.

b. Both mirror mounts are removed, and are replaced by cardboard discs with pinholes in their centers.

c. The Helium-Neon laser is set up on a laboratory stand. Its output is screened by a pinhole. It is positioned so that the alignment beam is directed into the plasma tube from the output end, through the pinholes at either end of the tube.

d. The disc is removed from the left (closed) end of the tube and the flat mirror and end cap are installed. The mirror is adjusted so that the alignment beam is reflected back to the pinhole in the output end. The alignment beam spreads somewhat, and the reflected spot will be larger than the pinhole.

e. The disc is removed from the right (output) end of the tube and the concave output mirror and KCl output window are installed. The alignment beam now enters the plasma tube through the output window and the output hole in the concave mirror. The output mirror is adjusted to direct the reflected alignment beam back to the flat

mirror. The flat mirror cannot be seen from the outside, so the reflection must be "walked" down the tube wall until it can no longer be seen. By "rocking" the adjustment, the alignment beam can be placed on the flat mirror.

f. When placed in operation according to the operating procedure of Appendix A, the laser should oscillate. The final mirror alignment can be made by optimizing the power output.

BIBLIOGRAPHY

1. Patel, C.K.N., "Continuous-Wave Laser Action on Vibrational-Rotational Transitions of CO₂," Physical Review, v. 136-5A, Nov. 1964.
2. Patel, C.K.N., "Selective Excitation Through Vibrational Energy Transfer and Optical Maser Action in N₂-CO₂," Physical Review Letters, v. 13-21, 23 Nov. 1964.
3. Patel, C.K.N. et al., "CW High-Power CO₂-N₂-He Laser," Applied Physics Letters, v. 7-11, Dec. 1965.
4. Cheo, P.K., "CO₂ Lasers," Lasers, v. 3, Edited by Albert K. Levine, Marcel Dekker, Inc, 1971.
5. Patel, C.K.N., "High-Power Carbon Dioxide Lasers," Scientific American, v. 219, Aug. 1968.
6. Naval Postgraduate School Report, NPS-57G071101A, The CO₂-HN₃ Laser, by D.J. Collins and G.P. Schnez, June 1971.
7. Forsyth, J.M., "Recent Developments in Gas Laser Technology," Society of Photo-Optical Instrumentation Engineers Seminar Proceedings, v. 20, 1969.
8. Cheo, P.K., "Relaxation of CO₂ Laser Levels by Collisions with Foreign Gases," IEEE Journal of Quantum Electronics, v. QE-4-10, Oct. 1968.
9. Fowler, M.C., "Quantitative Analysis of the Dependence of CO₂ Laser Performance on Electric Discharge Properties," Applied Physics Letters, v. 18, Mar. 1971.
10. Sinclair, Douglas C. and Bell, W. Earl, Gas Laser Technology, Holt, Rinehart and Winston, 1969.
11. Cheo, P.K. and Cooper, H.G., "Gain Characteristics of CO₂ Laser Amplifiers at 10.6 Microns," IEEE Journal of Quantum Electronics, v. QE-3/2.